Experimental and Numerical Characterization of Damage and Application to Incremental Forming

PhD thesis presentation

Carlos Felipe Guzmán

Department ArGEnCo
University of Liège, Belgium

February 1st, 2016

Simple geometries

Cooking pots

Simple geometries

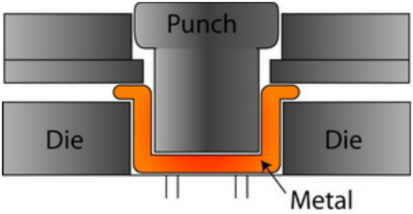

Manufactured by *Deep Drawing*

More complex geometries

Planes and car prototypes

More complex geometries

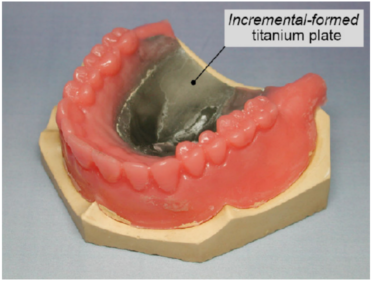

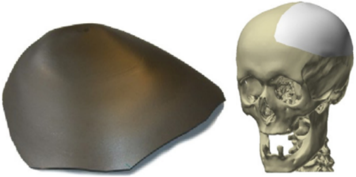

Implants

More complex geometries

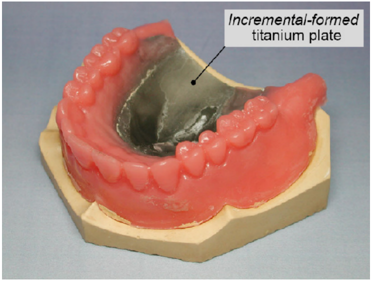

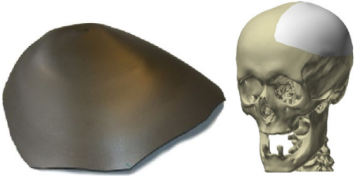

Implants

Manufactured by ???

Single point incremental forming
SPIF

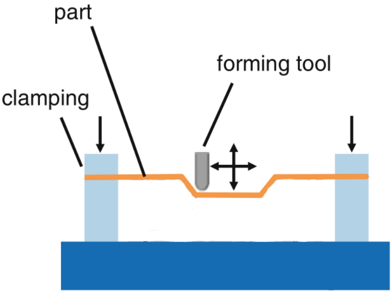

Hirt et al. [2015]

Schafer and Dieter Schraft [2005]

- A sheet metal is deformed by a small tool.
- The tool could be guided by a CNC (milling machine, robot).

Video

Single point incremental forming
SPIF

Advantages

- **Dieless**, with high sheet formability.
- Easy shape generation.
- For rapid prototypes, small batch productions, etc.

Single point incremental forming

SPIF

Advantages

- **Dieless**, with high sheet formability.
- Easy shape generation.
- For rapid prototypes, small batch productions, etc.

Challenges

- Poor geometrical accuracy.
- Process slowness.
- Characterization of service life.
- **The increased formability**.

The high formability of SPIF

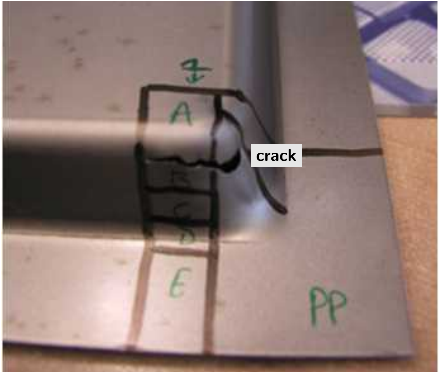

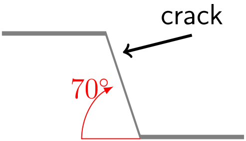

sine law:

$$t_f = t_0 \sin\alpha \Rightarrow t_f \approx 0.35$$

$$\epsilon \gg 1.0$$

The high formability of SPIF

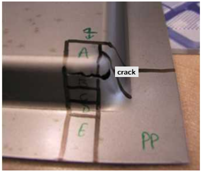

Detail:

$t_0 = 1.0\,\mathrm{mm}$

$t_f \approx 0.25\,\mathrm{mm}$

Forming Limit Curves

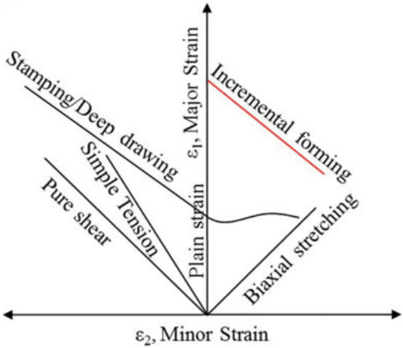

Reddy et al. [2015]

Methodology

Hypothesis

- The crack is preceded by damage.
- Damage is governed by microvoid nucleation, growth and coalescence.
- Damage is observed in SPIF [Lievers et al., 2004].

Methodology

Hypothesis

- The crack is preceded by damage.
- Damage is governed by microvoid nucleation, growth and coalescence.
- Damage is observed in SPIF [Lievers et al., 2004].

Tasks

1. Implementation of a damage model (Gurson) in the LAGAMINE FE code.
2. Identification of the material parameters of the damage model.
3. Evaluate the model to understand the process mechanics leading to fracture.

Thesis

Main question

Is the Gurson model with a shear extension able to predict failure in SPIF process?

Thesis

Main question

Is the Gurson model with a shear extension able to predict failure in SPIF process?

Objectives

- Efficient numerical model.
- Limitations of the **damage model** (if any).
- Reproduce the **SPIF process** mechanics.

Presentation contents

Contents

Constitutive modeling

- Elasticity

$$\boldsymbol{\epsilon} = \frac{1}{2G_s}\boldsymbol{\sigma} - \frac{\nu}{E}\frac{1}{3}\mathrm{tr}\left(\boldsymbol{\sigma}\right)\mathbf{I}$$

Constitutive modeling

- Elasticity

$$\boldsymbol{\epsilon} = \frac{1}{2G_s}\boldsymbol{\sigma} - \frac{\nu}{E}\frac{1}{3}\mathrm{tr}\left(\boldsymbol{\sigma}\right)\mathbf{I}$$

- Plasticity
  - Hill [1948] yield locus

$$F_p = \sqrt{\frac{1}{2}\left(\boldsymbol{\sigma} - \mathbf{X}\right) : \mathbb{H} : \left(\boldsymbol{\sigma} - \mathbf{X}\right)} - \sigma_Y\left(\bar{\epsilon}^P\right) = 0$$

  - Isotropic hardening: Swift law

$$\sigma_Y\left(\bar{\epsilon}^P\right) = K\left(\bar{\epsilon}^P + \epsilon_0\right)^n$$

  - Kinematic hardening: Armstrong and Fredrick [1966]

$$\dot{\mathbf{X}} = C_X\left(X_{\mathrm{sat}}\dot{\boldsymbol{\epsilon}}^P - \mathbf{X}\dot{\bar{\epsilon}}^P\right)$$

Constitutive modeling

- Elasticity

$$\boldsymbol{\epsilon} = \frac{1}{2G_s}\boldsymbol{\sigma} - \frac{\nu}{E}\frac{1}{3}\mathrm{tr}\left(\boldsymbol{\sigma}\right)\mathbf{I}$$

- Plasticity
  - Hill [1948] yield locus

$$F_p = \sqrt{\frac{1}{2}\left(\boldsymbol{\sigma} - \mathbf{X}\right) : \mathbb{H} : \left(\boldsymbol{\sigma} - \mathbf{X}\right)} - \sigma_Y\left(\bar{\epsilon}^P\right) = 0$$

  - Isotropic hardening: Swift law

$$\sigma_Y\left(\bar{\epsilon}^P\right) = K\left(\bar{\epsilon}^P + \epsilon_0\right)^n$$

  - Kinematic hardening: Armstrong and Fredrick [1966]

$$\dot{\mathbf{X}} = C_X\left(X_{\mathrm{sat}}\dot{\boldsymbol{\epsilon}}^P - \mathbf{X}\bar{\epsilon}^P\right)$$

- Damage ...

The damage model

Basic hypothesis

- Material deterioration that leads to material failure.
- Associated with the evolution of micro voids.

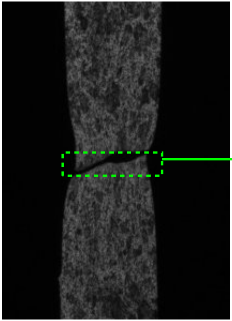

Cross section (2000x)

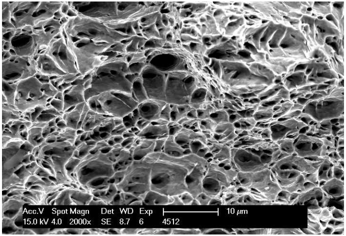

Anne Mertens, ULg

The damage model
Void evolution

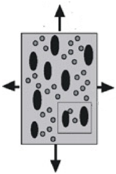

Base material

The damage model
Void evolution

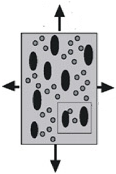

Base material

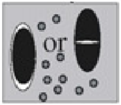

Nucleation

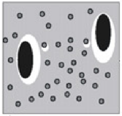

Growth

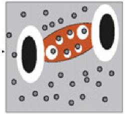

Coalescence

Lassance et al. [2007]

The Gurson [1977] model

Approach

- Micromechanics based yield criterion.
- Damage variable: void volume fraction (porosity).

$$F_p(\boldsymbol{\sigma}, f, \sigma_Y) = \frac{\sigma_{eq}^2}{{\sigma_Y}^2} - 1 + 2f \cosh\left(\frac{3}{2}\frac{\sigma_m}{\sigma_Y}\right) - f^2 = 0$$

The Gurson [1977] model

Approach

- Micromechanics based yield criterion.
- Damage variable: void volume fraction (porosity).

$$F_p(\boldsymbol{\sigma}, f, \sigma_Y) = \underbrace{\frac{\sigma_{eq}^2}{{\sigma_Y}^2} - 1}_{\text{Von Mises}} + 2f \cosh\left(\frac{3}{2}\frac{\sigma_m}{\sigma_Y}\right) - f^2 = 0$$

The Gurson [1977] model

Approach

- Micromechanics based yield criterion.
- Damage variable: void volume fraction (porosity).

$$F_p(\boldsymbol{\sigma}, f, \sigma_Y) = \frac{\sigma_{eq}^2}{{\sigma_Y}^2} - 1 + \underbrace{2f \cosh\left(\frac{3}{2}\frac{\sigma_m}{\sigma_Y}\right) - f^2}_{\text{Damage}} = 0$$

The Gurson [1977] model

Approach

- Micromechanics based yield criterion.
- Damage variable: void volume fraction (porosity).

$$F_p(\boldsymbol{\sigma}, \boxed{f}, \sigma_Y) = \underbrace{\frac{\sigma_{eq}^2}{{\sigma_Y}^2} - 1}_{\text{Von Mises}} + \underbrace{2\boxed{f}\cosh\left(\frac{3}{2}\frac{\sigma_m}{\sigma_Y}\right) - \boxed{f}^2}_{\text{Damage}} = 0$$

Matrix mass conservation:

$$\dot{f} = (1 - f)\, tr\dot{\epsilon}^p$$

1 material parameter:

$$f_0$$

GTN extension

The Gurson-Tvergaard-Needleman (GTN) extension:

- Nucleation [Chu and Needleman, 1980].
- Void growth (classical volumetric assumption).
- Coalescence [Tvergaard and Needleman, 1984].

$$\dot{f} = \dot{f}_{nucleation} + \dot{f}_{growth}$$

GTN extension
Tvergaard [1982]

$$F_p(\boldsymbol{\sigma}, f^*, \overline{\sigma}) = \underbrace{\frac{\sigma_{eq}^2}{\overline{\sigma}^2} - 1}_{\text{Von Mises}} + \underbrace{2q_1 f^* \cosh\left(-\frac{3}{2} q_2 \frac{\sigma_m}{\overline{\sigma}}\right) - q_3 \left(f^*\right)^2}_{\text{Damage}} = 0$$

GTN extension

Tvergaard [1982]

$$F_p(\boldsymbol{\sigma}, f^*, \epsilon_M^P) = \underbrace{\frac{\sigma_{eq}^2}{\sigma_Y^2} - 1}_{\text{Von Mises}} + \underbrace{2\boxed{q_1} f^* \cosh\left(-\frac{3\boxed{q_2}\sigma_m}{2\sigma_Y}\right) - \boxed{q_3}(f^*)^2}_{\text{Damage}} = 0$$

Matrix hardening:

$$\sigma_Y = \sigma_Y(\epsilon_M^P)$$

2 material parameters:

$$q_1,\ q_2\ (q_3 = {q_1}^2)$$

Nucleation

Chu and Needleman [1980]

$$\dot{f} = \dot{f}_{nucleation} + \dot{f}_{growth}$$

$$\dot{f}_{nucleation} = \underbrace{\mathcal{A}\dot{\epsilon}_M^P}_{\text{Strain}} + \underbrace{\mathcal{B}\left(\dot{\sigma}_{eq} + c\dot{\sigma}_M\right)}_{\text{Stress}}$$

Nucleation
Chu and Needleman [1980]

$$\dot{f} = \dot{f}_{nucleation} + \dot{f}_{growth}$$

$$\dot{f}_{nucleation} = \underbrace{\mathcal{A}\dot{\epsilon}_M^P}_{\text{Strain}} + \underbrace{\mathcal{B}\left(\dot{\sigma}_{eq} + c\dot{\sigma}_M\right)}_{\text{Stress}}$$

$$\mathcal{A}(\epsilon_M^P) = \frac{1}{\sqrt{2\pi}}\frac{f_N}{S_N}\exp\left[-\frac{1}{2}\left(\frac{\epsilon_M^P - \epsilon_N}{S_N}\right)^2\right]$$

$$\mathcal{B}(\boldsymbol{\sigma}) = 0$$

Nucleation
Chu and Needleman [1980]

$$\dot{f} = \dot{f}_{nucleation} + \dot{f}_{growth}$$

$$\dot{f}_{nucleation} = \underbrace{\mathcal{A}\dot{\epsilon}_M^P}_{\text{Strain}} + \underbrace{\mathcal{B}\left(\dot{\sigma}_{eq} + c\dot{\sigma}_M\right)}_{\text{Stress}}$$

$$\mathcal{A}(\epsilon_M^P) = \frac{1}{\sqrt{2\pi}}\frac{\boxed{f_N}}{\boxed{S_N}}\exp\left[-\frac{1}{2}\left(\frac{\epsilon_M^P - \boxed{\epsilon_N}}{\boxed{S_N}}\right)^2\right]$$
$$\mathcal{B}(\boldsymbol{\sigma}) = 0$$

3 material parameters:

$$f_N,\ \epsilon_N,\ S_N$$

Coalescence
Tvergaard and Needleman [1984]

$$f^* = \begin{cases} f & \text{if } f < f_{cr} \\ f_{cr} + K_f(f - f_{cr}) & \text{if } f > f_{cr} \end{cases}$$

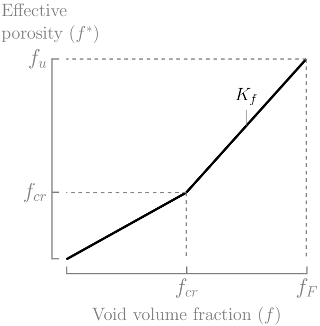

$$K_f = \frac{f_u - f_{cr}}{f_F - f_{cr}}$$

Coalescence
Tvergaard and Needleman [1984]

$$f^* = \begin{cases} f & \text{if } f < f_{cr} \\ f_{cr} + K_f(f - f_{cr}) & \text{if } f > f_{cr} \end{cases}$$

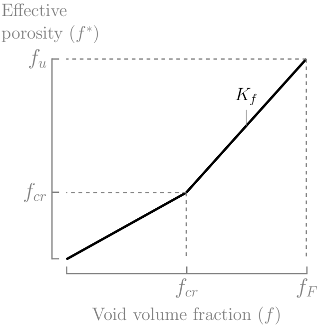

$$K_f = \frac{f_u - \boxed{f_{cr}}}{\boxed{f_F} - \boxed{f_{cr}}}$$

2 material parameters:

$$f_{cr},\ f_F \ \left(f_u = \frac{1}{q_1} \right)$$

Shear extensions

- Coupling of stress and damage history.
- Triaxiality: measure of the stress state.

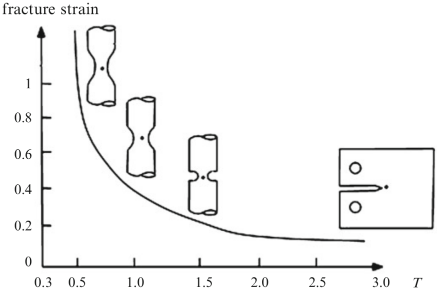

[Pineau and Pardoen, 2007]

Shear extensions

- Coupling of stress and damage history.
- Triaxiality: measure of the stress state.

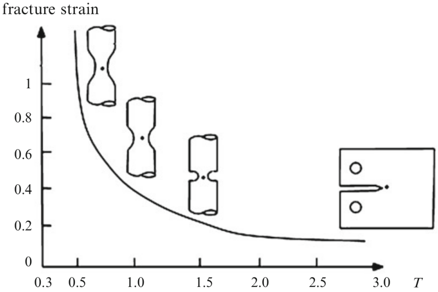

[Pineau and Pardoen, 2007]

$$T(I_1, J_2) = \frac{\sigma_m}{\sigma_{eq}}$$

$$T \to 0 \Longrightarrow \epsilon_f \to \infty$$

Shear extensions
Failure modes

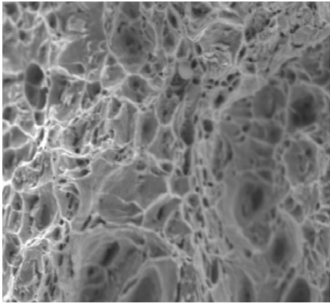

Cavity controlled ($T = 1.10$)

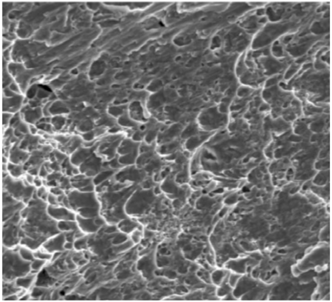

Shear controlled($T = 0.47$)

[Barsoum and Faleskog, 2007]

Shear extensions
Failure modes

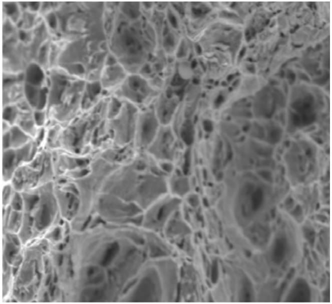

Cavity controlled ($T = 1.10$)

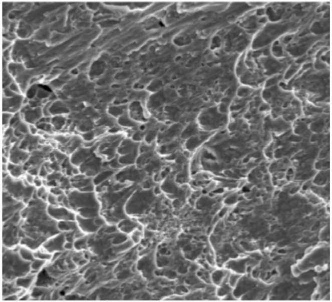

Shear controlled($T = 0.47$)

[Barsoum and Faleskog, 2007]

- GTN model $\rightarrow$ No damage is predicted when $T = 0$.
- At low triaxiality, void shape evolution becomes important.

Shear extensions

Nahshon and Hutchinson [2008]

$$\dot{f} = \dot{f}_g + \dot{f}_n + \dot{f}_{shear}$$

$$\dot{f}_{shear} = \boxed{k_\omega} f \omega(\boldsymbol{\sigma}) \frac{\boldsymbol{\sigma}_{dev} : \dot{\boldsymbol{\epsilon}}^P}{\sigma_{eq}}$$

Shear extensions

Nahshon and Hutchinson [2008]

$$\dot{f} = \dot{f}_g + \dot{f}_n + \dot{f}_{shear}$$

$$\dot{f}_{shear} = \boxed{k_\omega} f \omega(\boldsymbol{\sigma}) \frac{\boldsymbol{\sigma}_{dev} : \dot{\boldsymbol{\epsilon}}^P}{\sigma_{eq}}$$

1 material parameter: k_ω.

Note: $\omega(\boldsymbol{\sigma})$ is a scalar functions of the stress.

Contents

Numerical implementation

- Based on Ben Bettaieb et al. [2011b,a]
- Complete GTN model:
    - Kinematic hardening (classical non-linear).
    - Nucleation and coalescence (GTN model).
    - Shear [Nahshon and Hutchinson, 2008].

Numerical implementation

- Based on Ben Bettaieb et al. [2011b,a]
- Complete GTN model:
  - Kinematic hardening (classical non-linear).
  - Nucleation and coalescence (GTN model).
  - Shear [Nahshon and Hutchinson, 2008].
  - Matrix anisotropy (Hill type) [Benzerga and Besson, 2001]:

$$\widetilde{q} = \sqrt{\frac{1}{2}\left(\boldsymbol{\sigma} - \mathbf{X}\right) : \mathbb{H} : \left(\boldsymbol{\sigma} - \mathbf{X}\right)}$$

Integration scheme

Equations set

$$F_p(\boldsymbol{\sigma}, \mathbf{X}, \mathbf{H}) = 0$$

$$d\boldsymbol{\epsilon}^P = d\lambda \frac{\partial F_p}{\partial \boldsymbol{\sigma}}$$

$$d\mathbf{H} = h(d\boldsymbol{\epsilon}^P, \boldsymbol{\sigma}, \mathbf{H})$$

Integration scheme

Equations set

$$F_p(\boldsymbol{\sigma}, \mathbf{X}, \mathbf{H}) = 0$$

$$d\boldsymbol{\epsilon}^P = d\lambda \frac{\partial F_p}{\partial \boldsymbol{\sigma}}$$

$$d\mathbf{H} = h(d\boldsymbol{\epsilon}^P, \boldsymbol{\sigma}, \mathbf{H})$$

Backward Euler
Aravas [1987]

$$\boldsymbol{\epsilon}_{n+1} = \boldsymbol{\epsilon}_n + \Delta t \dot{\boldsymbol{\epsilon}}_{n+1}$$

$$\Delta t = t_{n+1} - t_n$$

Integration scheme

Equations set

$$F_p(\boldsymbol{\sigma}, \mathbf{X}, \mathbf{H}) = 0$$

$$d\boldsymbol{\epsilon}^P = d\lambda \frac{\partial F_p}{\partial \boldsymbol{\sigma}}$$

$$d\mathbf{H} = h(d\boldsymbol{\epsilon}^P, \boldsymbol{\sigma}, \mathbf{H})$$

Backward Euler
Aravas [1987]

$$\boldsymbol{\epsilon}_{n+1} = \boldsymbol{\epsilon}_n + \Delta t \dot{\boldsymbol{\epsilon}}_{n+1}$$

$$\Delta t = t_{n+1} - t_n$$

Ben Bettaieb et al. [2011b]

$$\Gamma(\mathbf{Y}) = 0$$

$$Y_i = \left\{ \Delta\epsilon_p, \Delta\epsilon_q, n_1, n_2, n_3, n_4, n_5, \epsilon_M^P, f \right\}$$

Integration scheme

Equations set

$$F_p(\boldsymbol{\sigma}, \mathbf{X}, \mathbf{H}) = 0$$

$$d\boldsymbol{\epsilon}^P = d\lambda \frac{\partial F_p}{\partial \boldsymbol{\sigma}}$$

$$d\mathbf{H} = h(d\boldsymbol{\epsilon}^P, \boldsymbol{\sigma}, \mathbf{H})$$

Backward Euler
Aravas [1987]

$$\boldsymbol{\epsilon}_{n+1} = \boldsymbol{\epsilon}_n + \Delta t \dot{\boldsymbol{\epsilon}}_{n+1}$$

$$\Delta t = t_{n+1} - t_n$$

Ben Bettaieb et al. [2011b]

$$\Gamma(\mathbf{Y}) = 0$$

$$Y_i = \left\{ \Delta\epsilon_p, \Delta\epsilon_q, n_1, n_2, n_3, n_4, n_5, \epsilon_M^P, f \right\}$$

N-R iteration

$$\Gamma_i + \sum_{j=1}^{9} \frac{\partial \Gamma_i}{\partial Y_j} dY_j = 0$$

Numerical validation
Hydrostatic test Nahshon and Xue [2009]

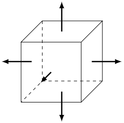

Gurson parameters

q_1	1.0	f_N	0.04	f_0	0.005
q_2	1.0	ϵ_N	0.30	f_c	0.15
q_3	1.0	S_N	0.10	f_f	0.25

Numerical validation
Hydrostatic test Nahshon and Xue [2009]

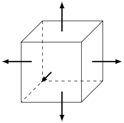

Gurson parameters

q_1	1.0	f_N	0.04	f_0	0.005
q_2	1.0	ϵ_N	0.30	f_c	0.15
q_3	1.0	S_N	0.10	f_f	0.25

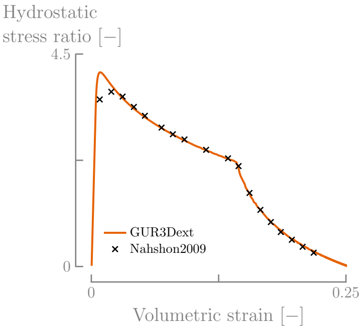

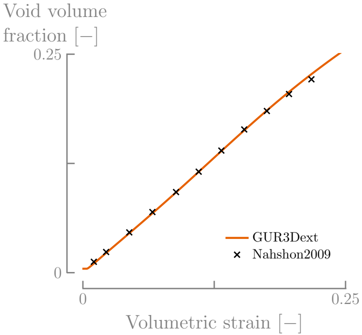

Numerical validation

Shear test Nahshon and Xue [2009]

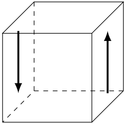

Gurson parameters

q_1	1.0	f_N	0.04	f_0	0.005
q_2	1.0	ϵ_N	0.30	f_c	0.15
q_3	1.0	S_N	0.10	f_f	0.25

Numerical validation
Shear test Nahshon and Xue [2009]

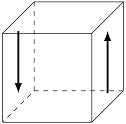

Gurson parameters					
q_1	1.0	f_N	0.04	f_0	0.005
q_2	1.0	ϵ_N	0.30	f_c	0.15
q_3	1.0	S_N	0.10	f_f	0.25

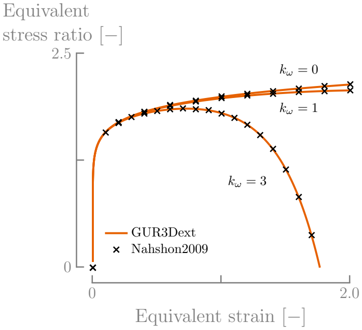

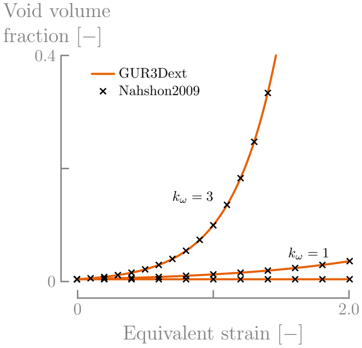

Contents

Material presentation

- DC01 ferritic steel (EN 10330).
- 1.0 mm thickness.

Microstructure:

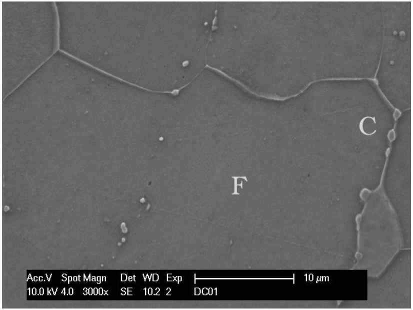

Anne Mertens, ULg

Mn	C	Al	Ni,Cu,Cr,P
0.21	0.049	0.029	<0.025

Experimental setup

Uniaxial Zwick machine

Load capacity: $\pm 100\,\mathrm{kN}$

Bi-axial machine

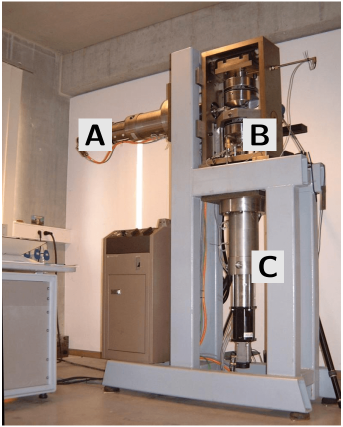

Digital Image Correlation
DIC

- Contactless method for displacements and strains.
- Pattern tracking.

CMOS cameras, resolution 1280x800

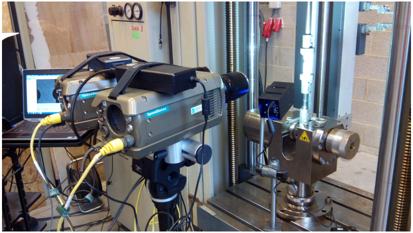

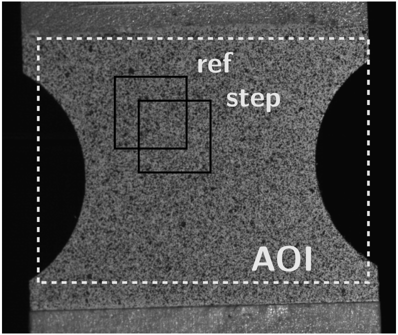

Tensile

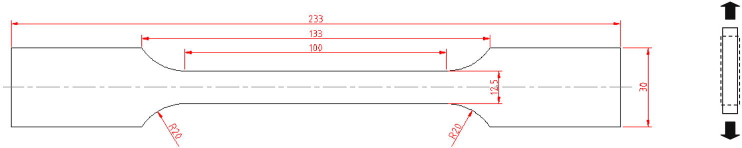

Shear

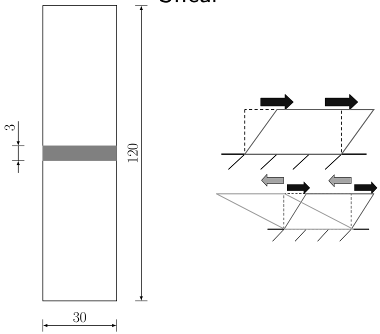

Plane strain

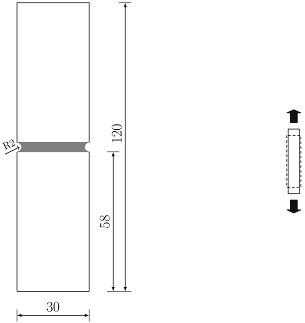

Plasticity tests

Tensile and shear test

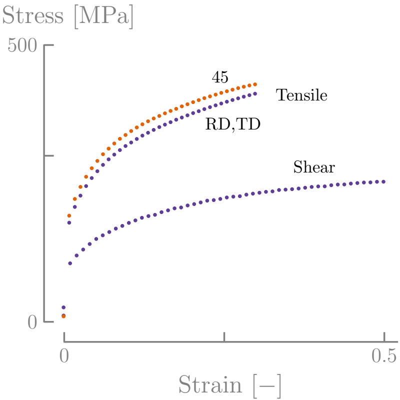

Plasticity tests

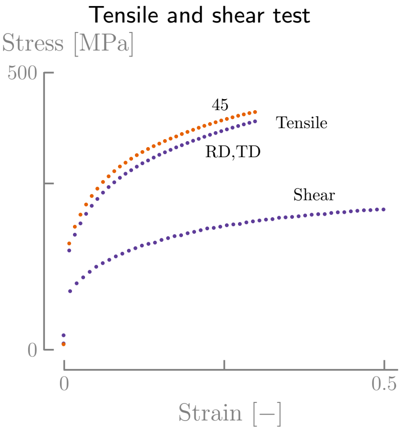

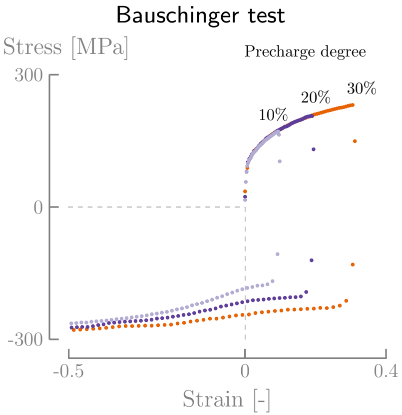

Plasticity tests

Tensile and shear test

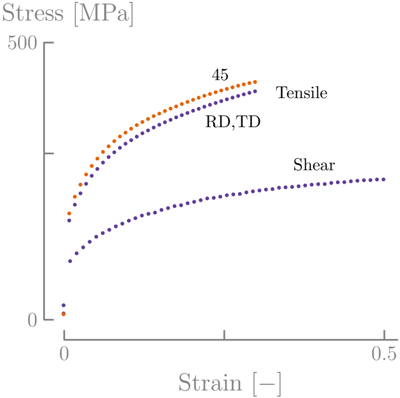

Bauschinger test

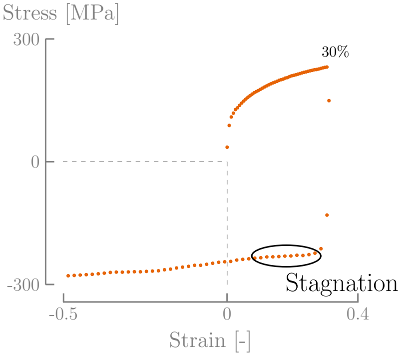

Identification of material parameters

- Hill [1948] parameters $\rightarrow$ Classical simulated annealing.
- Hardening (K, n, ϵ_0, C_x, X_{sat}) $\rightarrow$ Inverse optimization (OPTIM).

$$\text{error norm} = \sqrt{\sum_{i=1}^{N} \left(y_i^{\text{FE}} - y_i^{\text{exp}}\right)^2}$$

Identification of material parameters

- Hill [1948] parameters $\rightarrow$ Classical simulated annealing.
- Hardening (K, n, ϵ_0, C_x, X_{sat}) $\rightarrow$ Inverse optimization (OPTIM).

$$\text{error norm} = \sqrt{\sum_{i=1}^{N} \left(y_i^{\mathrm{FE}} - y_i^{\exp}\right)^2}$$

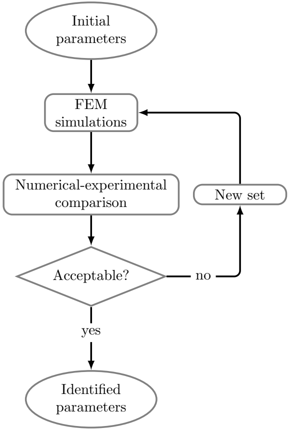

Identification of material parameters

Tensile test

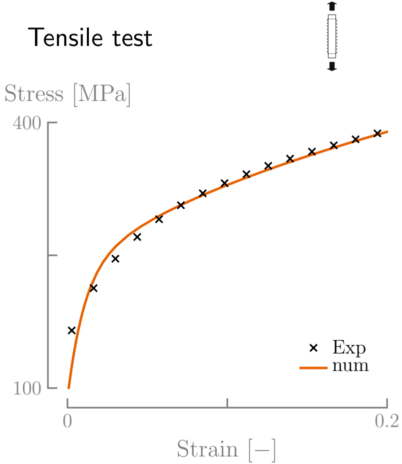

Identification of material parameters

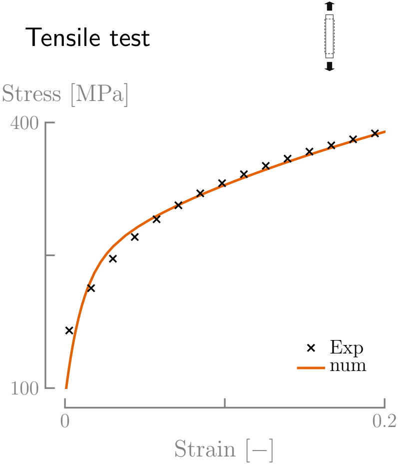

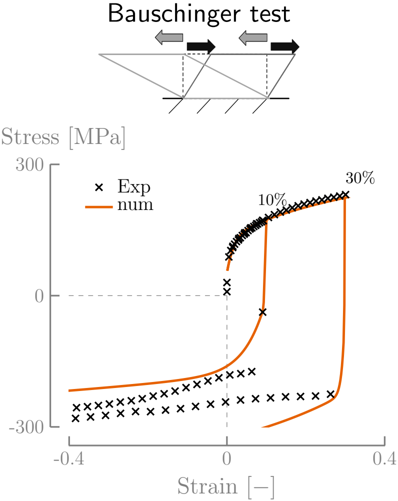

Contents

GTN characterization

Methodology

Difference with plasticity

- Microscopic scale, heterogeneous deformation.
- Force vs. displacement instead of stress vs. strain.
- Coupling between variables.

GTN characterization
Methodology

Difference with plasticity

- Microscopic scale, heterogeneous deformation.
- Force vs. displacement instead of stress vs. strain.
- Coupling between variables.

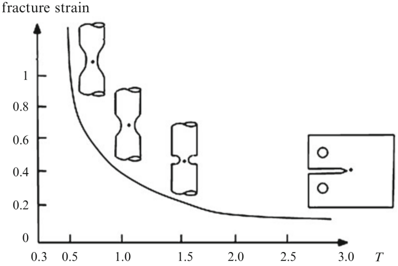

GTN parameters characterization

Automatic optimization (OPTIM) issues

- CPU time, iterations, etc.
- Sensitivity of nucleation, coalescence parameters.
- Introduction of weights in the error norm.

GTN parameters characterization

Automatic optimization (OPTIM) issues

- CPU time, iterations, etc.
- Sensitivity of nucleation, coalescence parameters.
- Introduction of weights in the error norm.

Approach:

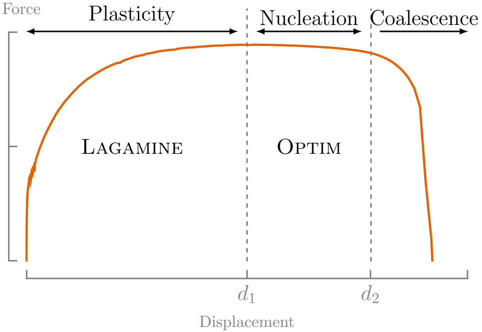

Macroscopic test campaign

$R = 5$

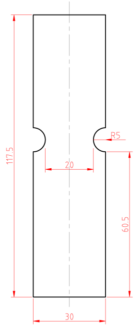

$T \approx$0.6-0.7

$\omega \approx$0.25-0.4

$R = 10$

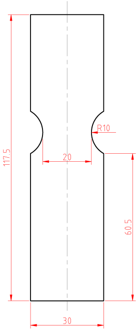

$T \approx$0.5-0.7

$\omega \approx$0.2-0.4

hole

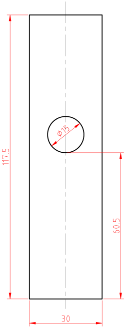

$T \approx$0.35-0.6

$\omega \approx$0.0

shear

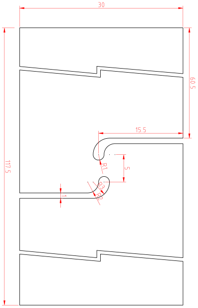

$T \approx$0.0

$\omega \approx$1.0

Force predictions

Set name			Nucleation		Coalescence		Shear
	f_0	f_N	ϵ_N	S_N	f_c	f_F	k_ω
set1					0.0055	0.135	0.25
set2	0.0008	0.0025	0.175	0.42	0.0045	0.145	0.25
set3					0.0025	0.170	0.075

Force predictions

Set name		*Nucleation*			*Coalescence*		*Shear*
	f_0	f_N	ϵ_N	S_N	f_c	f_F	k_ω
set1					0.0055	0.135	0.25
set2	0.0008	0.0025	0.175	0.42	0.0045	0.145	0.25
set3					0.0025	0.170	0.075

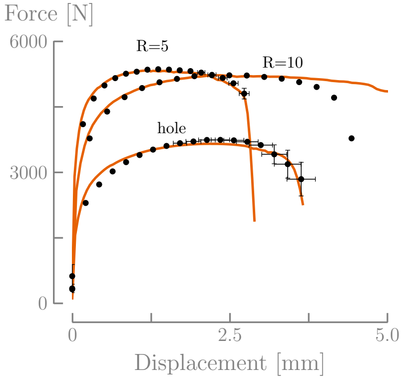

Force predictions

Set name	f_0	f_N	ϵ_N	S_N	f_c	f_F	k_ω
	Nucleation				*Coalescence*		*Shear*
set1					0.0055	0.135	0.25
set2	0.0008	0.0025	0.175	0.42	0.0045	0.145	0.25
set3					0.0025	0.170	0.075

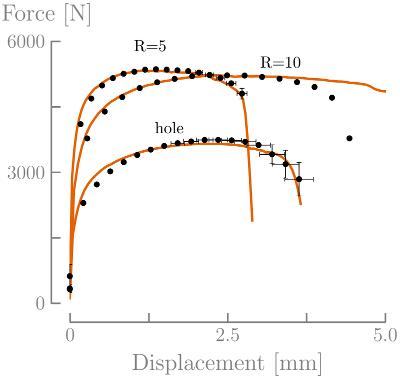

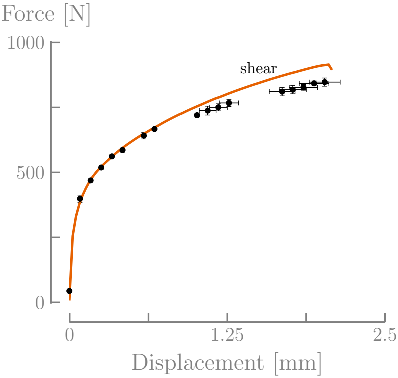

Strain prediction

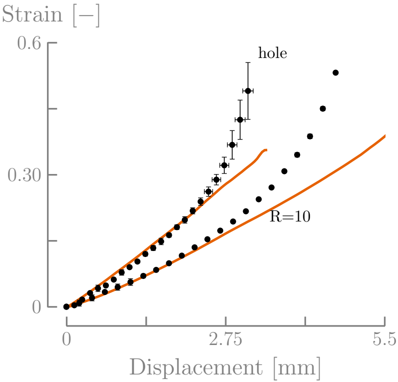

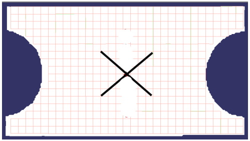

Strain localization is not captured

Strain prediction

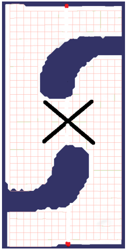

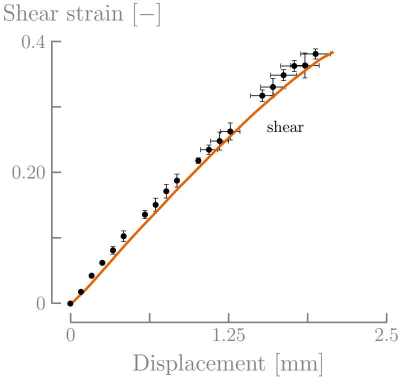

DIC vs. FE predictions

Axial strain

	DIC	Numerical
notch $R = 5$	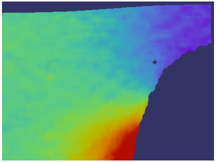	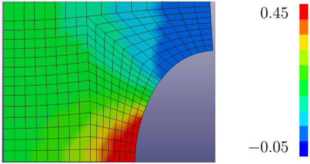
notch $R = 10$	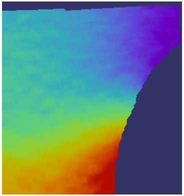	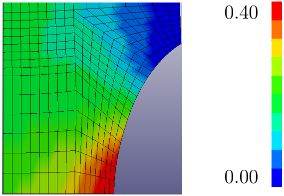

DIC vs. FE predictions

Axial strain

	DIC	Numerical
hole	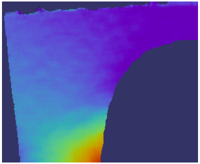	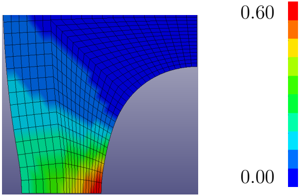
shear	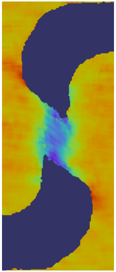	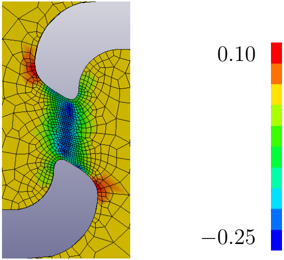

Discussion

Results

- Loss on load carrying capacity is captured.
- Strain localization is not captured.
- Limitations of the GTN model.

Source of errors

- Parameters q_1 and q_2 were not calibrated.
- Hardening stagnation.
- Mesh sensitivity.

Contents

Literature review summary

Simulate SPIF is not easy

- Small contact zone with a very long path.
- High strains.
- Incremental deformation, simulation time.
- Sensitivity of force prediction to FE choice, constitutive law.
- Boundary conditions, grip modeling.

Literature review summary
Shape inaccuracies

- Springback, bending.
- Elastic strains.

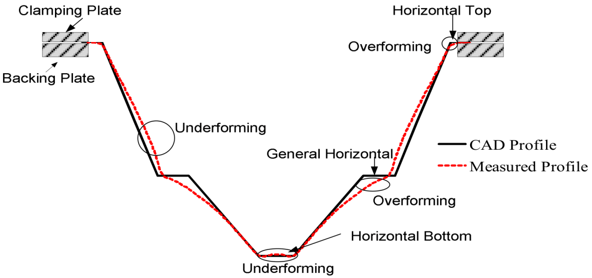

Literature review summary
Formability

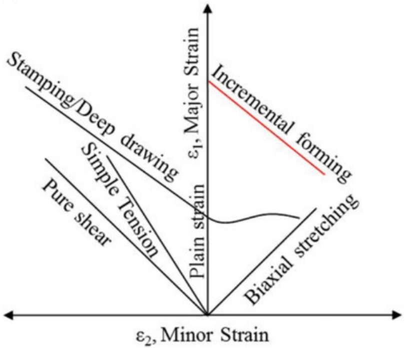

- Forming Limit Curve (FLC): classic approach.
- Through the thickness shear, Bending-under-tension, cyclic effects, etc.

Literature review summary
Damage

Definition

Mechanism of degradation leading to fracture (Damage $\neq$ formability)

Definition

Mechanism of degradation leading to fracture (Damage $\neq$ formability)

Malhotra et al. [2012].

- Shear itself cannot explain higher fomability:
- Early localization: Noodle theory.

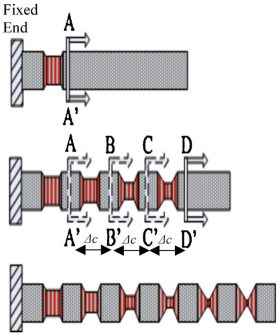

Finite element type

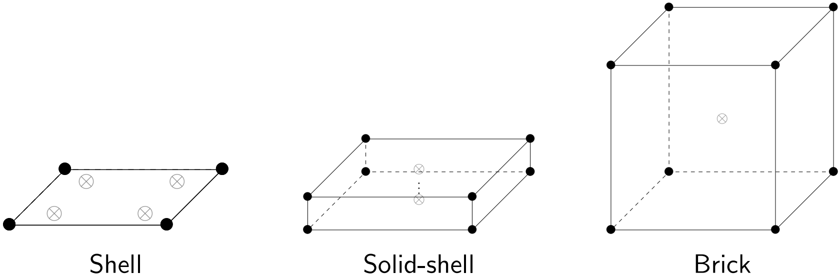

Finite element type

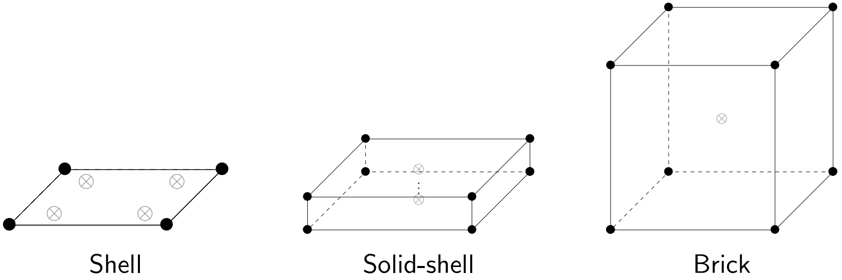

- RESS solid-shell element [Alves de Sousa, 2006].
- Numerical technique: Enhanced assumed strain (EAS)

$$\boldsymbol{\epsilon} = \boldsymbol{\epsilon}^{\mathsf{com}} + \boldsymbol{\epsilon}^{\mathsf{EAS}}$$

Line test
Description

- Most basic SPIF test.
- Experimental data by Hans Vanhove (KULeuven).

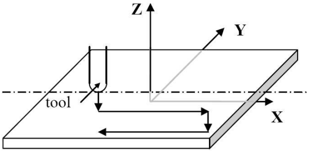

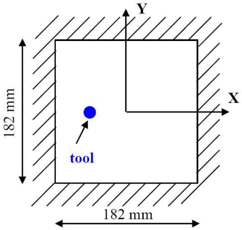

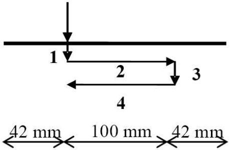

Numerical-Experimental validation

Shape: top and bottom surface

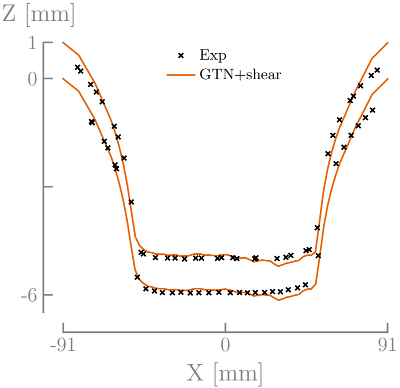

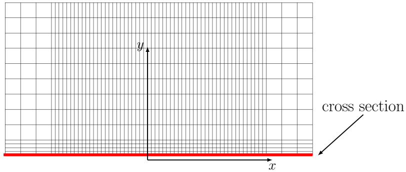

Numerical-Experimental validation

Shape: top and bottom surface

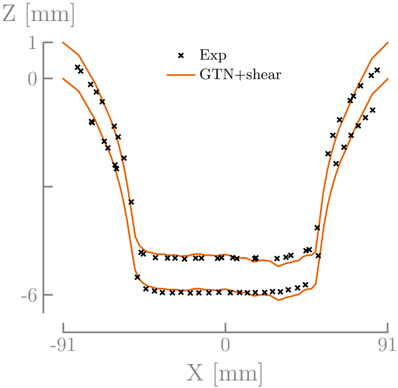

Force

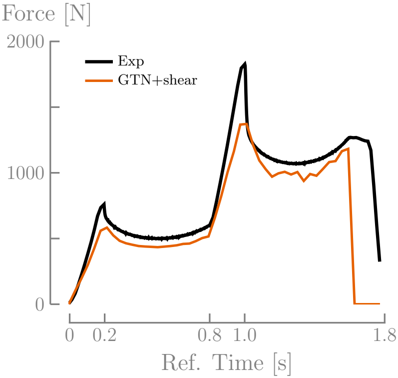

Two-slope pyramid
Description

- For shape accuracy assessment.
- Experimental DIC shape by Amar Behera (KULeuven).

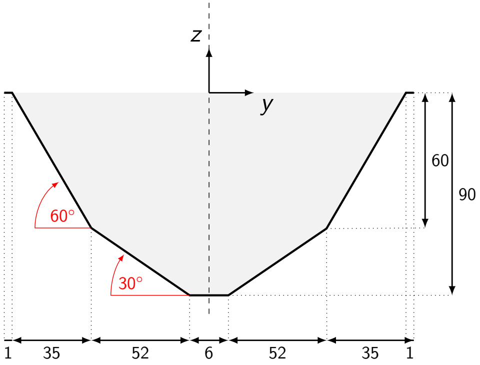

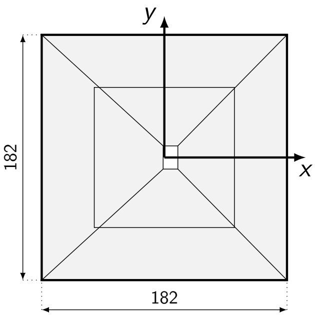

Numerical predictions
Experimentally there is no crack!

Shape: bottom surface

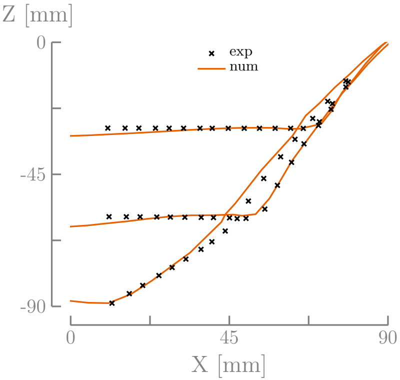

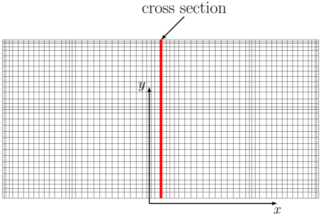

Numerical predictions
Experimentally there is no crack!

Shape: bottom surface

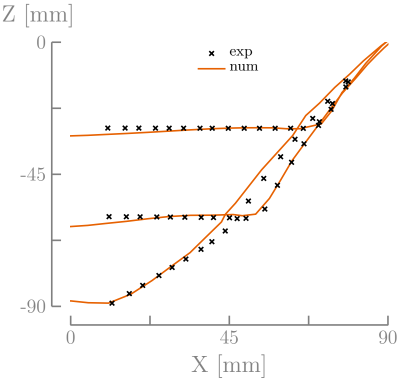

Forces: no experiments available

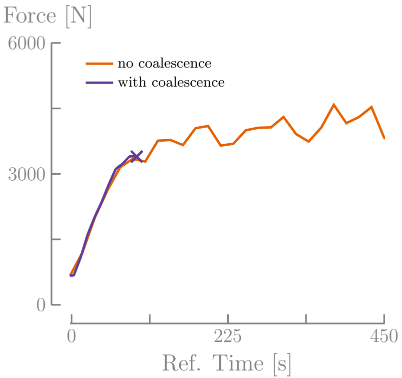

With coalescence, the model predicts fracture. . . prematurely

Cone test
Description

- Benchmark for failure angles.
- DC01, 1.0 mm $\Rightarrow \alpha =$67°

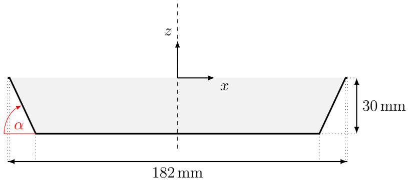

DC01 steel, 1.0 mm
$\Rightarrow$ failure angle: 67°

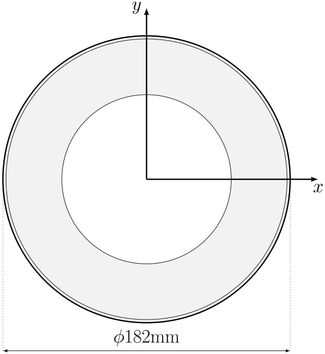

Numerical predictions

Force prediction (no experiments)

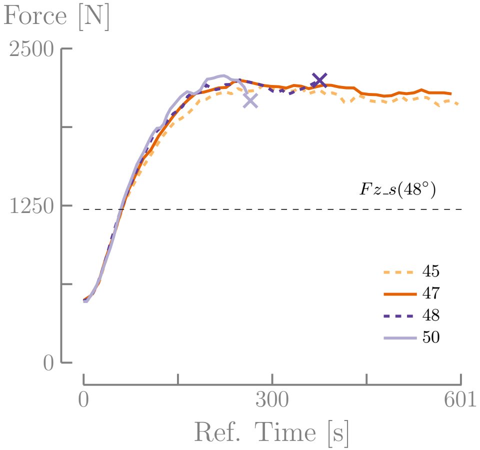

The crack is predicted at $\alpha = 48°$

Numerical predictions

Force prediction (no experiments)

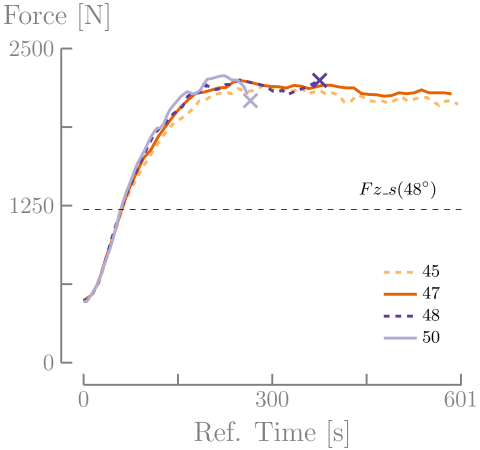

Aerens et al. [2009] formula:

$$Fz\_s = 0.0716 R_m t^{1.57} {d_t}^{0.41} \Delta h^{0.09}$$
$$\ldots (\alpha - d\alpha) \cos(\alpha - d\alpha)$$

$\alpha = 47^\circ$	1219.70 N
$\alpha = 48^\circ$	1222.49 N
$\alpha = 67^\circ$	1158.01 N

The crack is predicted at $\alpha = 48^\circ$

Analysis of fracture prediction

1. Predicted force overestimation.
2. Bad modeling of the deformation.
3. Limitations of the GTN model.

Analysis of fracture prediction

1. Predicted force overestimation.
2. Bad modeling of the deformation.
3. Limitations of the GTN model.

Porosity for the 47° cone

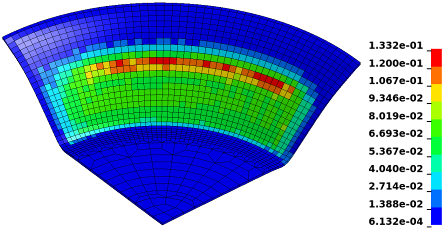

no fracture

Porosity for the 48° cone

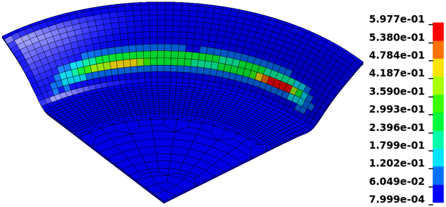

$\epsilon_f \approx 0.8$

Contents

Conclusions

Contributions

- Fully implicit implementation of the GTN+shear model.
- Extensive experimental data and material identification.
- Good shape prediction in SPIF (FE element type).

Conclusions

Contributions

- Fully implicit implementation of the GTN+shear model.
- Extensive experimental data and material identification.
- Good shape prediction in SPIF (FE element type).

Issues

- **The chosen damage model is capable to predict failure in the SPIF process but not accurately**.
- GTN model uncouples the hardening and damage.
- Force prediction in SPIF.

Perspectives

- Modification of the hardening in the GTN model [Leblond et al., 1995].
- Implement different type of damage model [Lemaitre, 1985; Xue, 2007].
- Effect of hardening stagnation on damage.

Perspectives

- Modification of the hardening in the GTN model [Leblond et al., 1995].
- Implement different type of damage model [Lemaitre, 1985; Xue, 2007].
- Effect of hardening stagnation on damage.

SPIF

- Remeshing + Damage in LAGAMINE.
- Different EAS modes solid-shell.

Experimental and Numerical Characterization of Damage and Application to Incremental Forming

PhD thesis presentation

Carlos Felipe Guzmán

Department ArGEnCo
University of Liège, Belgium

February 1st, 2016

- Incomplete pole figures:

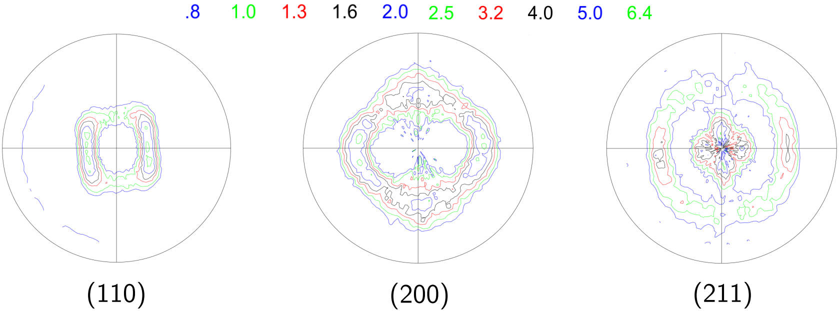

Philip Eyckens, KULeuven

Shear extensions

Xue [2008]

$$f^* \rightarrow D$$

$$\dot{D} = K_f \left(q_1 \dot{f} + \dot{D}_{shear} \right)$$

$$\dot{D}_{shear} = \boxed{k_g} f^{1/3} g_\theta(\boldsymbol{\sigma}) \epsilon_{eq} \dot{\epsilon}_{eq}$$

Shear extensions

Xue [2008]

$$f^* \to D$$

$$\dot{D} = K_f \left(q_1 \dot{f} + \dot{D}_{shear} \right)$$

$$\dot{D}_{shear} = \boxed{k_g} f^{1/3} g_\theta(\boldsymbol{\sigma}) \epsilon_{eq} \dot{\epsilon}_{eq}$$

Nahshon and Hutchinson [2008]

$$\dot{f} = \dot{f}_g + \dot{f}_n + \dot{f}_{shear}$$

$$\dot{f}_{shear} = \boxed{k_\omega} f \omega(\boldsymbol{\sigma}) \frac{\boldsymbol{\sigma}_{dev} : \dot{\boldsymbol{\epsilon}}^P}{\sigma_{eq}}$$

Shear extensions

Xue [2008]

$$f^* \to D$$

$$\dot{D} = K_f \left(q_1 \dot{f} + \dot{D}_{shear} \right)$$

$$\dot{D}_{shear} = \boxed{k_g} f^{1/3} g_\theta(\boldsymbol{\sigma}) \epsilon_{eq} \dot{\epsilon}_{eq}$$

Nahshon and Hutchinson [2008]

$$\dot{f} = \dot{f}_g + \dot{f}_n + \dot{f}_{shear}$$

$$\dot{f}_{shear} = \boxed{k_\omega} f \omega(\boldsymbol{\sigma}) \frac{\boldsymbol{\sigma}_{dev} : \dot{\boldsymbol{\epsilon}}^P}{\sigma_{eq}}$$

1 material parameter: k_g or k_ω.

Note: $g_\theta(\boldsymbol{\sigma})$ and $\omega(\boldsymbol{\sigma})$ are scalar functions of the stress.

Integration scheme

Consistent tangent matrix, algorithm approach

$$\boldsymbol{\sigma} = \boldsymbol{\sigma}(\boldsymbol{\epsilon})$$

$$d\boldsymbol{\sigma} = \mathbb{D} : d\boldsymbol{\epsilon} \quad ; \qquad \mathbb{D} := \frac{\partial \boldsymbol{\sigma}}{\partial \boldsymbol{\epsilon}}$$

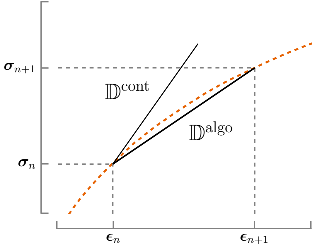

$$\boldsymbol{\sigma} = \boldsymbol{\sigma}(\boldsymbol{\epsilon})$$

$$d\boldsymbol{\sigma} = \mathbb{D} : d\boldsymbol{\epsilon} \quad ; \qquad \mathbb{D} := \frac{\partial \boldsymbol{\sigma}}{\partial \boldsymbol{\epsilon}}$$

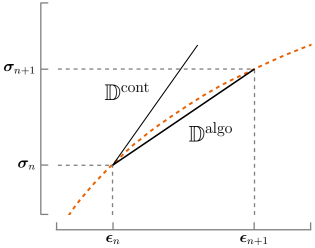

$$\boldsymbol{\sigma}_{n+1} = \mathbb{C} : \left(\boldsymbol{\epsilon}_{n+1} - \boldsymbol{\epsilon}^P_{n+1}\right)$$

Linearization

$$d\boldsymbol{\sigma} = \mathbb{C} : d\boldsymbol{\epsilon} - \mathbb{C} : d\Delta\boldsymbol{\epsilon}^P$$

Relate $d\boldsymbol{\epsilon}$ with $d\Delta\boldsymbol{\epsilon}^P$

Integration scheme
Consistent tangent matrix, algorithm approach

$$\boldsymbol{\sigma} = \boldsymbol{\sigma}(\boldsymbol{\epsilon})$$

$$d\boldsymbol{\sigma} = \mathbb{D} : d\boldsymbol{\epsilon} \quad ; \qquad \mathbb{D} := \frac{\partial \boldsymbol{\sigma}}{\partial \boldsymbol{\epsilon}}$$

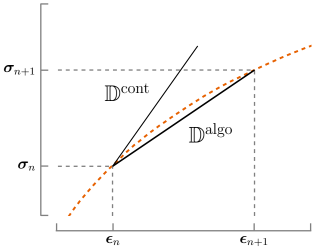

$$\mathbb{K} : \partial \Delta \boldsymbol{\epsilon}^P = \mathbb{L} : \partial \boldsymbol{\sigma}$$

Kim and Gao [2005] approach

$$\mathbb{D} = \mathbb{C} - \mathbb{C}(\mathbb{K} + \mathbb{L}\mathbb{C})^{-1}\mathbb{L}\mathbb{C}$$

$$\frac{\partial F_p}{\partial \boldsymbol{\sigma}}, \frac{\partial F_p}{\partial \Delta \boldsymbol{\epsilon}^{\mathbf{P}}}, \frac{\partial F_p}{\partial H_\beta}, \frac{\partial^2 F_p}{\partial \boldsymbol{\sigma}^2}, \frac{\partial^2 F_p}{\partial \boldsymbol{\sigma} \partial \Delta \boldsymbol{\epsilon}^P}, \ldots$$

Extension to Kinematic hardening

Numerical validation

Hydrostatic test, Aravas [1987]

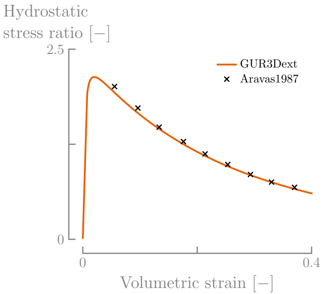

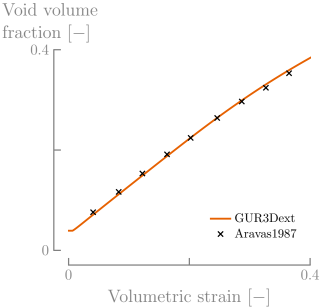

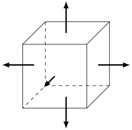

Elasto-plastic parameters				Gurson parameters					
E	210 GPa	K	1200 MPa	q_1	1.5	f_N	0.04	f_0	0
ν	0.3	ϵ_0	3.17×10^{-3}	q_2	1.0	ϵ_N	0.30	f_c	-
		n	0.1	q_3	2.25	S_N	0.10	f_f	-

Tensile test
Aravas [1987]

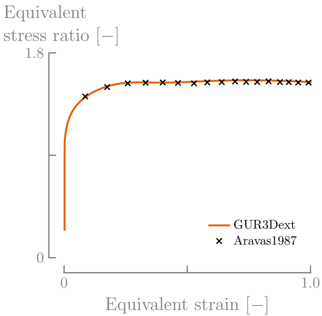

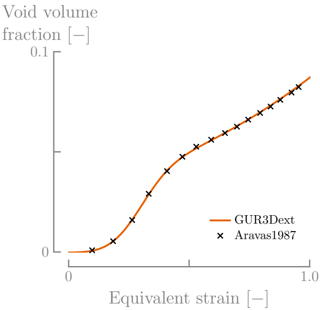

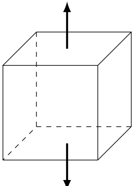

Elasto-plastic parameters				Gurson parameters					
E	210 GPa	K	1200 MPa	q_1	1.5	f_N	0.04	f_0	0
ν	0.3	ϵ_0	3.17×10^{-3}	q_2	1.0	ϵ_N	0.30	f_c	-
		n	0.1	q_3	2.25	S_N	0.10	f_f	-

Numerical validation
Shear test Xue [2008]

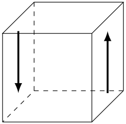

Gurson parameters

q_1	1.5	f_N	0.04	f_0	0.00
q_2	1.0	ϵ_N	0.20	f_c	0.05
q_3	2.25	S_N	0.10	f_f	0.25

Numerical validation
Shear test Xue [2008]

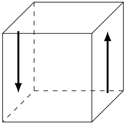

Gurson parameters

q_1	1.5	f_N	0.04	f_0	0.00
q_2	1.0	ϵ_N	0.20	f_c	0.05
q_3	2.25	S_N	0.10	f_f	0.25

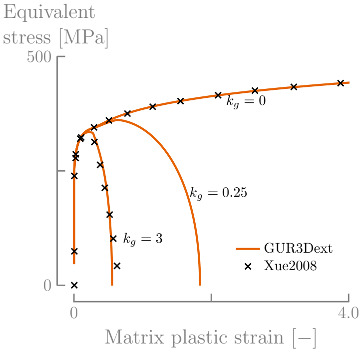

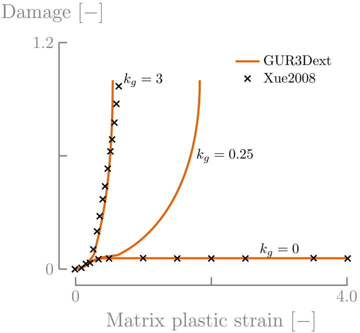

State variables analysis

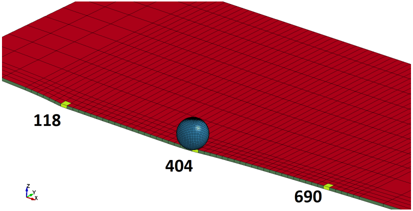

State variables analysis

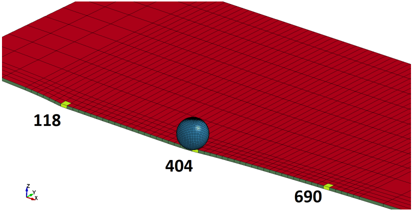

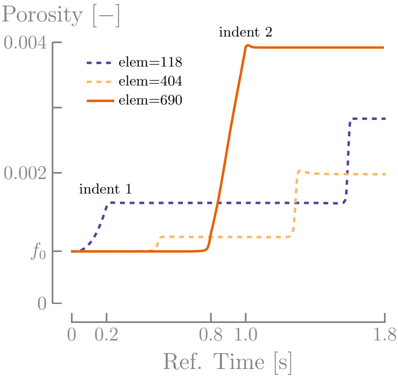

SPIF line test
State variables analysis

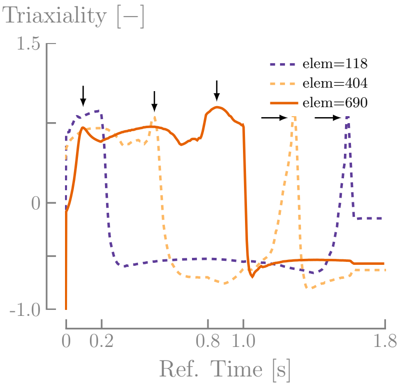

SPIF line test
State variables analysis

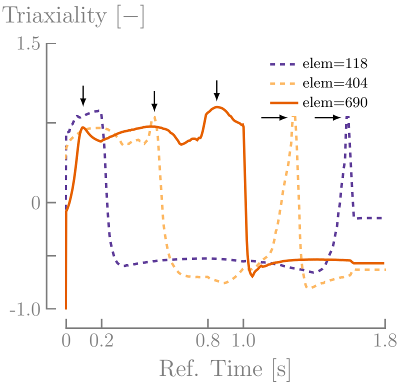

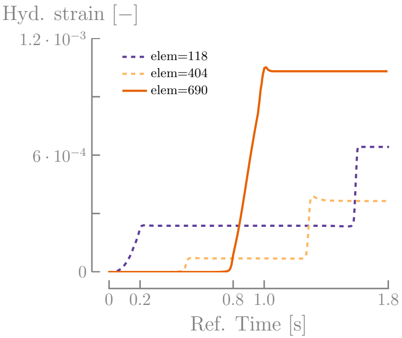

SPIF Two-slope pyramid
Mesh and boundary conditions

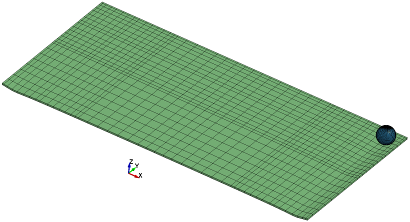

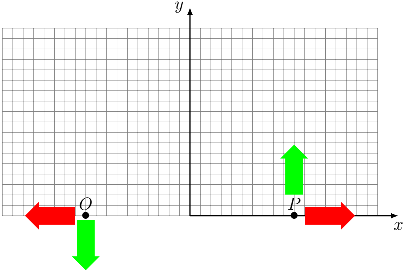

$$(u_x)_O = -(u_x)_P$$
$$(u_y)_O = -(u_y)_P$$
$$(u_z)_O = (u_z)_P$$

SPIF Two-slope pyramid
Numerical predictions

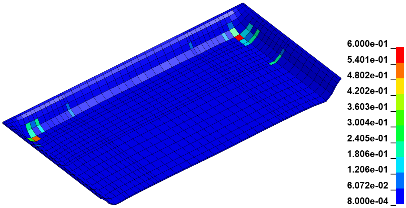

Porosity f

SPIF Two-slope pyramid
Numerical predictions

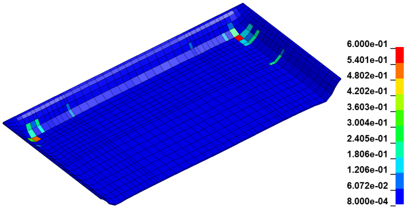

Porosity f

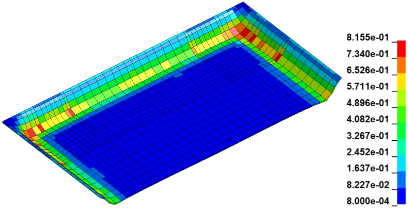

Eq. macro. strain ϵ_q

Cone test

Mesh and boundary conditions

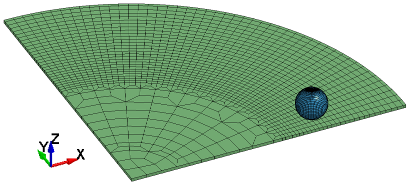

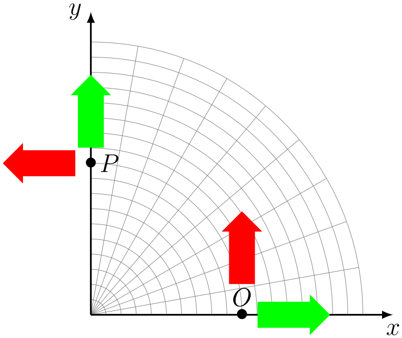

References I

Aerens, R., Eyckens, P., van Bael, A., Duflou, J., 2009. Force prediction for single point incremental forming deduced from experimental and FEM observations. The International Journal of Advanced Manufacturing Technology 46 (9-12), 969–982.

Alves de Sousa, R. J., 2006. Development of a General Purpose Nonlinear Solid- Shell Element and its Application to Anisotropic Sheet Forming Simulation. Phd thesis, Universidade de Aveiro.

Aravas, N., 1987. On the numerical integration of a class of pressure-dependent plasticity models. International Journal for Numerical Methods in Engineering 24 (7), 1395–1416.

Armstrong, P., Fredrick, C., 1966. A Mathematical Representation of the Multiaxial Bauschinger Effect. Technical report, Central Electricity Generating Board.

Barsoum, I., Faleskog, J., 2007. Rupture mechanisms in combined tension and shear-Experiments. International Journal of Solids and Structures 44 (6), 1768–1786.

Ben Bettaieb, M., Lemoine, X., Bouaziz, O., Habraken, A. M., Duchêne, L., 2011a. Numerical modeling of damage evolution of DP steels on the basis of X-ray tomography measurements. Mechanics of Materials 43 (3), 139–156.

Ben Bettaieb, M., Lemoine, X., Duchêne, L., Habraken, A. M., 2011b. On the numerical integration of an advanced Gurson model. International Journal for Numerical Methods in Engineering 85 (8), 1049–1072.

Benzerga, A. A., Besson, J., 2001. Plastic potentials for anisotropic porous solids. European Journal of Mechanics - A/Solids 20 (3), 397–434.

References II

Chu, C. C., Needleman, A., 1980. Void Nucleation Effects in Biaxially Stretched Sheets. Journal of Engineering Materials and Technology 102 (3), 249.

Gurson, A. L., 1977. Continuum theory of ductile rupture by void nucleation and growth: Part I-Yield criteria and flow rules for porous ductile media. Journal of Engineering Materials and Technology 99 (1), 2–15.

Hill, R., may 1948. A Theory of the Yielding and Plastic Flow of Anisotropic Metals. Proceedings of the Royal Society A: Mathematical, Physical and Engineering Sciences 193 (1033), 281–297.

Hirt, G., Bambach, M., Bleck, W., Prahl, U., Stollenwerk, J., 2015. The Development of Incremental Sheet Forming from Flexible Forming to Fully Integrated Production of Sheet Metal Parts. In: Brecher, C. (Ed.), Advances in Production Technology. Lecture Notes in Production Engineering. Springer International Publishing, Cham, Ch. 9, pp. 117–129.

Kim, J., Gao, X., 2005. A generalized approach to formulate the consistent tangent stiffness in plasticity with application to the GLD porous material model. International Journal of Solids and Structures 42 (1), 103–122.

Lassance, D., Fabregue, D., Delannay, F., Pardoen, T., 2007. Micromechanics of room and high temperature fracture in 6xxx Al alloys. Progress in Materials Science 52 (1), 62–129.

Leblond, J.-B., Perrin, G., Devaux, J., 1995. An improved Gurson-type model for hardenable ductile metals. European journal of mechanics. A. Solids 14 (4), 499–527.

Lemaitre, J., 1985. A Continuous Damage Mechanics Model for Ductile Fracture. Journal of Engineering Materials and Technology 107 (1), 83.

References III

Lievers, W., Pilkey, A., Lloyd, D., 2004. Using incremental forming to calibrate a void nucleation model for automotive aluminum sheet alloys. Acta Materialia 52 (10), 3001–3007.

Malhotra, R., Xue, L., Belytschko, T., Cao, J., 2012. Mechanics of fracture in single point incremental forming. Journal of Materials Processing Technology 212 (7), 1573–1590.

Nahshon, K., Hutchinson, J. W., 2008. Modification of the Gurson Model for shear failure. European Journal of Mechanics - A/Solids 27 (1), 1–17.

Nahshon, K., Xue, Z., 2009. A modified Gurson model and its application to punch-out experiments. Engineering Fracture Mechanics 76 (8), 997–1009.

Pineau, A., Pardoen, T., 2007. Failure mechanisms of metals. Comprehensive structural integrity encyclopedia 2.

Reddy, N. V., Lingam, R., Cao, J., 2015. Incremental Metal Forming Processes in Manufacturing. In: Nee, A. Y. C. (Ed.), Handbook of Manufacturing Engineering and Technology. Springer London, London, Ch. 9, pp. 411–452.

Schafer, T., Dieter Schraft, R., dec 2005. Incremental sheet metal forming by industrial robots. Rapid Prototyping Journal 11 (5), 278–286.

Tvergaard, V., 1982. On localization in ductile materials containing spherical voids. International Journal of Fracture 18 (4), 237–252.

Tvergaard, V., Needleman, A., 1984. Analysis of the cup-cone fracture in a round tensile bar. Acta Metallurgica 32 (1), 157–169.

References IV

Xue, L., 2007. Damage accumulation and fracture initiation in uncracked ductile solids subject to triaxial loading. International Journal of Solids and Structures 44 (16), 5163–5181.

Xue, L., 2008. Constitutive modeling of void shearing effect in ductile fracture of porous materials. Engineering Fracture Mechanics 75 (11), 3343–3366.